www.sciencemag.org/content/348/6231/201/suppl/DC1

Supplementary Material for

The principle of antagonism ensures protein targeting specificity at the endoplasmic reticulum

Martin Gamerdinger, Marie Anne Hanebuth, Tancred Frickey, Elke Deuerling*

*Corresponding author. E-mail: elke.deuerling@uni-konstanz.de

Published 10 April 2015, *Science* **348**, 201 (2015)
DOI: 10.1126/science.aaa5335

This PDF file includes:

Materials and Methods
Figs. S1 to S7
Full Reference List

Materials and Methods

Strains

Caenorhabditis elegans was cultured according to standard techniques (*44*). SJ4005 (zcIs4[*hsp-4p::GFP*]), SJ4100 (zcIs13[*hsp-6p::GFP*]), TJ375 (gpls1[*hsp-16-2::GFP*]), SS104 [*glp-4*(*bn2*) I], CB4037 [*glp-1*(*e2141*) III] and N2 were obtained from the *Caenorhabditis* Genetics Center. To generate strains overexpressing NAC the coding sequences of *icd-1* (β-NAC) and *icd-2* (α-NAC) were amplified from N2 genomic DNA by PCR and inserted into a vector containing the *eft-3* promoter and the *tbb-2* 3′ untranslated region (UTR) sequence. DNA was injected into N2 worms at 5 ng/µl in the presence of *myo2p::mCherry* (5 ng/µl) and DNA ladder (100 ng/µl, GeneRuler 1 kb, Thermo Scientific). Control strains were obtained by injecting 10 ng/µl empty vector, 5 ng/µl *myo2p::mCherry* and 100 ng/µl DNA ladder. To obtain splitGFP expressing strains, spGFP1-10 and spGFP11 coding sequences were amplified from *CD4-2::spGFP1-10 and CD4-2::spGFP11* constructs (*45*) by PCR and cloned into a vector containing the *dpy-30* promoter and the *let-858* 3′ UTR. For localization in mitochondria and ER, the spGFP fragments were fused to N-terminal targeting sequences of Hsp-60 and Stc-1, respectively. A KDEL ER retention motif was added to the C-terminus of the ER-localized spGFP fragments. DNA was injected into N2 animals at 50 ng/µl together with rol-6 (pRF4, 100 ng/µl) (*46*) as the co-injection marker.

Isolation of cytosolic and membrane-attached ribosomes

The nematodes were grown in liquid culture and harvested on ice in 0.1 M NaCl supplemented with 300 µg/ml cycloheximide. After separation from the *E. coli* food source by sucrose floatation, the worms were frozen in liquid nitrogen and pellets ground to powder in a mortar. The powder was thawed on ice and resuspended in lysis buffer (30 mM HEPES pH 7.4, 75 mM KoAc, 5 mM $MgCl_2$, 5% (w/v) mannitol, 100 µg/ml cycloheximide, 2 mM β-mercaptoethanol, 1 × Complete protease inhibitor mix (Roche)) followed by centrifugation at 20.000 x g for 20 min at 4°C. The supernatant containing cytosolic ribosomes was collected and filtered through a 0.45 µm cellulose filter (Sartorius). The pellet was resuspended in lysis buffer supplemented with 0.008% (w/v) digitonin (Calbiochem), incubated for 5 min on ice and centrifuged again. After one additional washing step in lysis buffer membrane-attached ribosomes were released by incubating pellets in lysis buffer supplemented with 2% (v/v) NP40 for 30 min on ice. After centrifugation the supernatant containing membrane-attached ribosomes was collected and filtered through a 0.45 µm cellulose filter. The cytosolic and membrane fractions were then subjected to ribosome sedimentation or immunoblot analyses as described below.

To obtain a large homogenous population of control and NAC-overexpressing worms (carrying an extrachromosomal array) for polysome analyses, 30.000 transgenic L1s were sorted based on the pharyngeal mCherry fluorescence using the COPAS Biosorter (Union Biometrica).

Analysis of ribosome-associated mRNA distribution

Cytosolic and membrane fractions were subjected to sucrose density gradient centrifugation and polysome recording as described (*18*). Fractions containing mono- and

polysomes were collected and RNA was extracted using RNeasy mini columns (Qiagen). For the experiments shown in Figures 3G and 4C polysomal fractions (disome to tetrasome) were pooled and the extracted RNA was subjected to quantitative RT-PCR using 18s rRNA as an internal standard. For the experiments shown in Figures 4A-B all ribosomal fractions (monosome to tetrasome) were pooled and the extracted RNA was analyzed using dual-color (Cy3 and Cy5) 8x60K Agilent *C. elegans* microarrays (OakLabs). Probe preparation, microarray hybridization and detection were performed by OakLabs according to their standard protocols. Analyses were performed in quadruplicates.

Analysis of microarray data

The microarray files were imported into 'R' [R-project.org] using the 'bioconductor' and 'limma' packages [both at bioconductor.org]. The data were normalized within each array using the 'loess' method and probe sets measuring differentially expressed genes were identified by fitting linear models and performing an empirical Bayes analysis of these models (eBayes R-module). Comparison of the empty vector control datasets (membrane-bound vs. cytosolic fractions) returned 13247 probe sets indicating significantly ($P<0.05$) differentially expressed mRNAs (of 52326 quantifiable probe sets).

Figure 4A: For the probe sets differentially enriched in the empty vector control experiment, we were able to extract the corresponding protein sequences from 'wormbase' [wormbase.org] for 2466 genes showing an enrichment in the membrane fraction and 1176 genes showing an enrichment in the cytosolic fraction. These protein sequences were then analysed using SignalP [SignalP 4.0: discriminating signal peptides from transmembrane regions, doi: 10.1038/nmeth.1701] and TMHMM2 (*47*) to identify probably signal sequences as well as transmembrane regions.

Figure 4B: Linear regressions were calculated using the 'lm()' method in 'R' and the formula 'y~x'. All data points of significantly enriched probe sets in control animals (empty vector, ev) were plotted along the X-axis and colored according to the predicted localization of encoded proteins. Predictions were performed as in Fig. 4A. The corresponding values for the NAC RNAi datasets were plotted on the Y-axis. To make the datasets comparable, all measurements for the NAC RNAi membrane-enriched fraction had to be multiplied with a factor of 2.19 due to a change in the membrane-to-cytosol ratio of ribosomes in NAC RNAi animals (see Fig. S6C, D).

Isolation of glycosylated proteins

Frozen worm pellets were ground to powder in a mortar on dry ice. The powder was resuspended in lysis buffer (10 mM Tris pH 7.4, 150 mM NaCl, 1 mM $CaCl_2$, 1 mM $MnCl_2$, 1 × Complete protease inhibitor mix), centrifuged at 20.000 x g for 20 min at 4°C, filtered through a 0.45 µm cellulose filter and centrifuged again. This extraction method releases the majority of ER luminal proteins (tested for Hsp-4 and Pdi-3), thus mild detergent extraction is not necessary (in fact we recommend omitting detergents like 0.5% NP40 as it strongly decreases binding of glycosylated proteins to the lectin). Samples were adjusted to identical protein concentrations (15 µg/µl) and 100 µl Concanavalin A beads (Sigma) were incubated with 1 ml of sample overnight on an orbital shaker at 4°C. Lectin beads were washed five times with lysis buffer and

glycosylated proteins were eluted with 1 M Methyl-α-D-mannopyranoside (100 µl, Alfa Aesar) for 30 min at 18°C with constant shaking. When indicated, protein samples were treated with PNGase F (NEB) under nondenaturing reaction conditions according to the manufacturer's protocol. Predictions of N-glycosylation sites were performed with NetNGlyc 1.0.

In vitro ribosome-translocon binding analyses

Expression and purification of *C. elegans* NAC was performed essentially as described previously (*18*). The ribosome-binding mutant $^{RRK/AAA}$NAC was generated by mutating the evolutionary conserved ^{29}RRK^{31} sequence motif (*34*) near the N-terminus of β-NAC (*icd-1*) to AAA using standard mutagenesis protocols.

Puromycin and high-salt stripped ribosomes (PKRibo) were purified from N2 worms. Frozen worm pellets were ground to a fine powder in a mortar on dry ice. The powder was resuspended in extraction buffer (300 mM Sorbitol, 20 mM HEPES pH 7.5, 1 mM EGTA, 5 mM $MgCl_2$, 10 mM KCl, 10% glycerol, 1 M KoAc, 1 mg/ml Puromycin, 1 × Complete protease inhibitor mix, 1 mM PMSF) and centrifuged at 20.000 x g for 20 min at 4°C. The supernatant was collected, filtered through a 0.45 µm cellulose filter and centrifuged again. Subsequently, sample was loaded onto a 20% sucrose cushion (2 x volume) prepared in extraction buffer and centrifuged at 200.000 x g for 4 h at 4°C. Pellet was rinsed two times and resuspended in extraction buffer overnight at 4°C with constant shaking. After a second purification on a sucrose cushion ribosomes were resuspended in extraction buffer, snap frozen in liquid N_2 and stored at -80°C.

Puromycin and high salt-stripped rough microsomes (PKRM) were prepared from temperature sensitive sterile mutants (CB4037). Frozen worms were ground to powder in a mortar and the powder was resuspended in lysis buffer (30 mM HEPES pH 7.4, 75 mM KoAc, 5 mM $MgCl_2$, 5% (w/v) mannitol, 2 mM β-mercaptoethanol, 1 × Complete protease inhibitor mix). Samples were sonicated (six pulses at level 2 and duty cycle 50%, Branson sonifier) for times on ice followed by centrifugation at 20.000 x g for 20 min at 4°C. Membrane pellets were resuspended in lysis buffer supplemented with 0.008% (w/v) digitonin (Calbiochem), incubated for 5 min on ice and centrifuged again. Membrane pellets were resuspended in PK-lysis buffer (50 mM HEPES pH 7.4, 1 M KoAc, 2.5 mM $MgoAc_2$, 1 mM DTT, 1 mM Puromycin, 1 × Complete protease inhibitor mix) and samples were again sonicated (four times) followed by centrifugation at 20.000 x g for 20 min at 4°C. Pelleted membranes were resuspended in PK-lysis buffer, incubated for additional 2 h at 25°C and pelleted again by centrifugation. PKRMs were washed once in reaction buffer (20 mM NaP pH 7.5, 120 mM NaCl, 6 mM $MgCl_2$, 2 mM DTT, 1 × Complete protease inhibitor mix), pelleted by centrifugation and resuspended in the same buffer to a final protein concentration of 15 µg/µl. PKRMs (75 µg protein) were then incubated in the presence and absence of PKRibos (0.5 µM) and purified WT-NAC or $^{RRK/AAA}$NAC (2 µM) for 2 h at 25°C with constant shaking in a total reaction volume of 35 µl (in reaction buffer). Subsequently, microsomes were again isolated by centrifugation. The supernatant containing unbound ribosomes was collected and the remaining pellet containing microsome-bound ribosomes was washed once in reaction buffer and then resuspended in 35 µl SDS lysis buffer (62.5 mM Tris pH 6.8, 1 mM EGTA, 2% SDS, 10% (w/v) sucrose). Equal volumes (10 µl) of both fractions were then subjected to SDS-PAGE and immunoblot analysis.

Native rough microsomes (RM) were prepared by resuspending worm powder in lysis buffer (30 mM HEPES pH 7.4, 75 mM KoAc, 5 mM $MgCl_2$, 5% (w/v) mannitol, 2 mM β-mercaptoethanol, 1 × Complete protease inhibitor mix) followed by sonication on ice (four times) and centrifugation at 20.000 x g for 20 min at 4°C. Membrane pellets were resuspended in lysis buffer supplemented with 0.008% (w/v) digitonin, incubated for 5 min on ice and centrifuged again. After one additional washing step in lysis buffer the native microsome fraction was resuspended in reaction buffer to a final protein concentration of 15 µg/µl. RMs (75 µg protein) were incubated in a 35 µl total reaction volume in the presence and absence of puromycin (1 mM) and purified WT-NAC or $^{RRK/AAA}$NAC (0.5 µM) for 2 h at 25°C with constant shaking. Subsequently, microsomes were re-isolated by centrifugation and the ribosome content in the pellet and supernatant fractions was assessed by immunoblotting as describe above.

Immunoblot analysis and antibodies

Protein samples were applied to SDS–PAGE and electroblotted onto a nitrocellulose membrane according to standard protocols. Signals in immunoblots were quantified using ImageJ software. Polyclonal antibody against *C. elegans* NAC was described previously (*18*). All other antibodies used throughout this study were Hsp-4 (Thermo Scientific, PA5-22967), Hsp-60 (DSHB), Pas-7 (DSHB, CePAS7), Actin (DSHB, JLA20), RPL-10 (Biomol, WA-AP17603a), Sec61α (Santa Cruz, sc-393182), Atp-2 (kind gift of W. Neupert) and Pdi-3 (kind gift of A. Page).

RNAi

RNAi was performed by feeding the worms with *E. coli* HT115(DE3) harboring the vector L4440 to express dsRNA of the respective genes. Simultaneous knockdown of two genes was achieved as described previously (*48*). If not noted otherwise, worms were subjected to SRP54, SRα and Sec61α RNAi at the L4/young adult stage to prevent developmental defects. All other RNAi treatments were started in the L1 stage.

qPCR

Total RNA was extracted from *C. elegans* using RNeasy mini columns (Qiagen) and cDNA was synthesized using the QuantiTect reverse transcription kit (Qiagen). qPCR was performed with GoTaq SybrGreen mix (Promega) using an ABI 7500 Fast Real-Time PCR system (Applied Biosystems). Data were analyzed using the comparative 2ΔΔCt method and *gpd-1* as a reference gene. Experiments were repeated at least three times.

Life span analyses

Life span analyses were performed at 20°C. Worms were grown on *E. coli* HT115(DE3) RNAi as a food source from hatch. One hundred animals were used per condition and scored every second day. All life span analyses were repeated at least three times.

Larval growth arrest analysis

Worms were grown at 20°C on *E. coli* HT115(DE3) RNAi as a food source from hatch and after four days the animals were scored whether or not they developed to

adults. At least 200 animals were used per condition and the analyses were repeated three times.

Fluorescence microscopy

For fluorescence microscopy, the worms were immobilized with sodium azide at specified ages, and fluorescence was assessed with a Zeiss Axio Imager A1 microscope. For analysis of the subcellular localization of spGFP fragments, the worms were anesthetized with 25 mM levamisole and fluorescence was assessed with a confocal laser-scanning microscope Leica TCS SP8.

References

44. S. Brenner, The genetics of *Caenorhabditis elegans*. *Genetics* **77**, 71-94 (1974).
45. E. H. Feinberg, M. K. Vanhoven, A. Bendesky, G. Wang, R. D. Fetter, K. Shen, C. I. Bargmann, GFP Reconstitution Across Synaptic Partners (GRASP) defines cell contacts and synapses in living nervous systems. *Neuron* **57**, 353-363 (2008).
46. C. C. Mello, J. M. Kramer, D. Stinchcomb, V. Ambros, Efficient gene transfer in *C. elegans*: extrachromosomal maintenance and integration of transforming sequences. *EMBO J.* **10**, 3959-3970 (1991).
47. A. Krogh, B. Larsson, G. von Heijne, E. L. Sonnhammer, Predicting transmembrane protein topology with a hidden Markov model: application to complete genomes. *J. Mol. Biol.* **305**, 567-580 (2001).
48. K. Min, J. Kang, J. Lee, A modified feeding RNAi method for simultaneous knock-down of more than one gene in *Caenorhabditis elegans*. *BioTechniques* 48, 229-232 (2010).

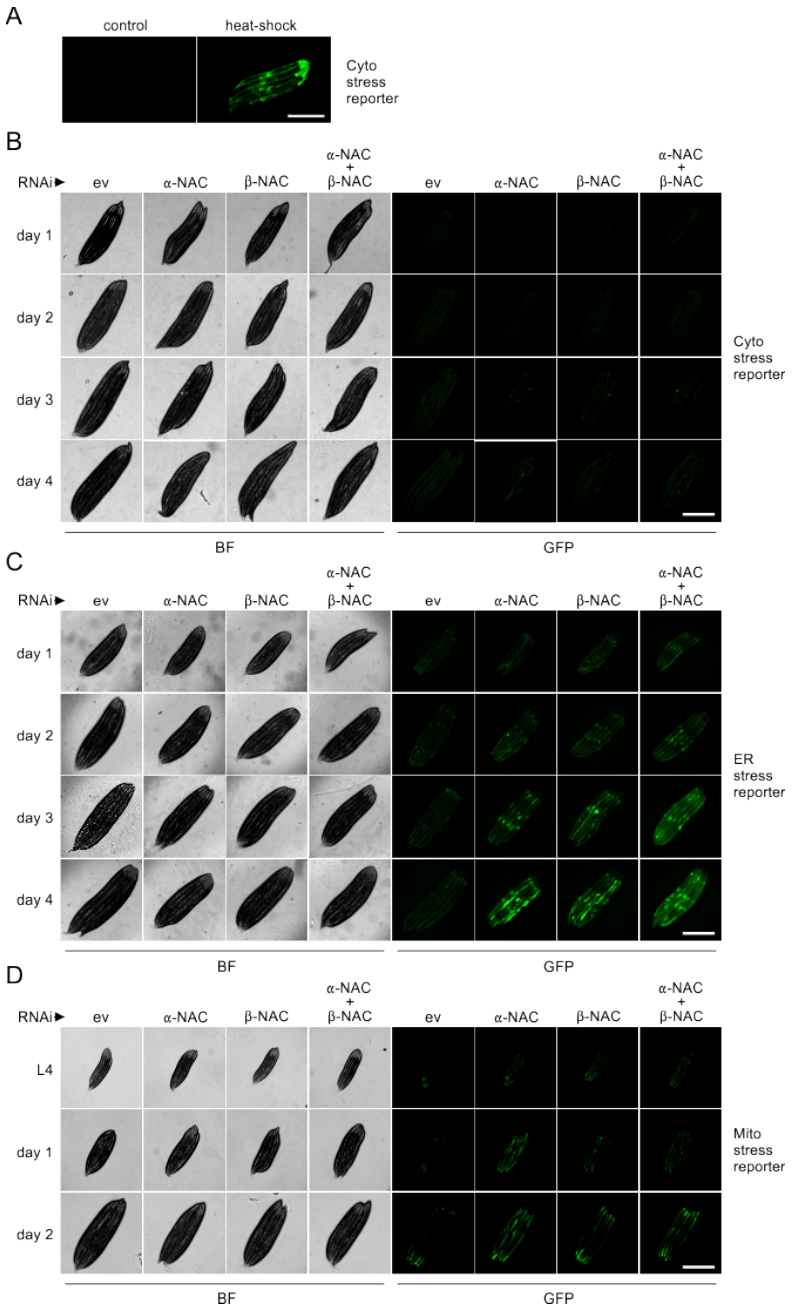

Fig. S1 NAC depletion induces ER and mitochondrial stress

(**A**) *hsp-16.2p::GFP* cytosolic stress reporter worms were heat-shocked for 90 min at 35°C and GFP fluorescence was assessed after 6 hours of recovery at 20°C. (**B**) *hsp-16.2p::GFP* cytosolic stress reporter worms were grown on empty vector control (ev) or indicated RNAi. GFP fluorescence was assessed from day 1 to day 4 of adulthood. (**C**) *hsp-4p::GFP* ER stress reporter worms were grown on empty vector control (ev) or indicated RNAi and GFP fluorescence was assessed from day 1 to day 4 of adulthood. (**D**) *hsp-6p::GFP* mitochondrial stress reporter worms were grown on empty vector control (ev) or indicated RNAi and GFP fluorescence was assessed from the last larval stage (L4) to day 2 of adulthood. BF = Bright-field. Scale bar = 0.5 mm.

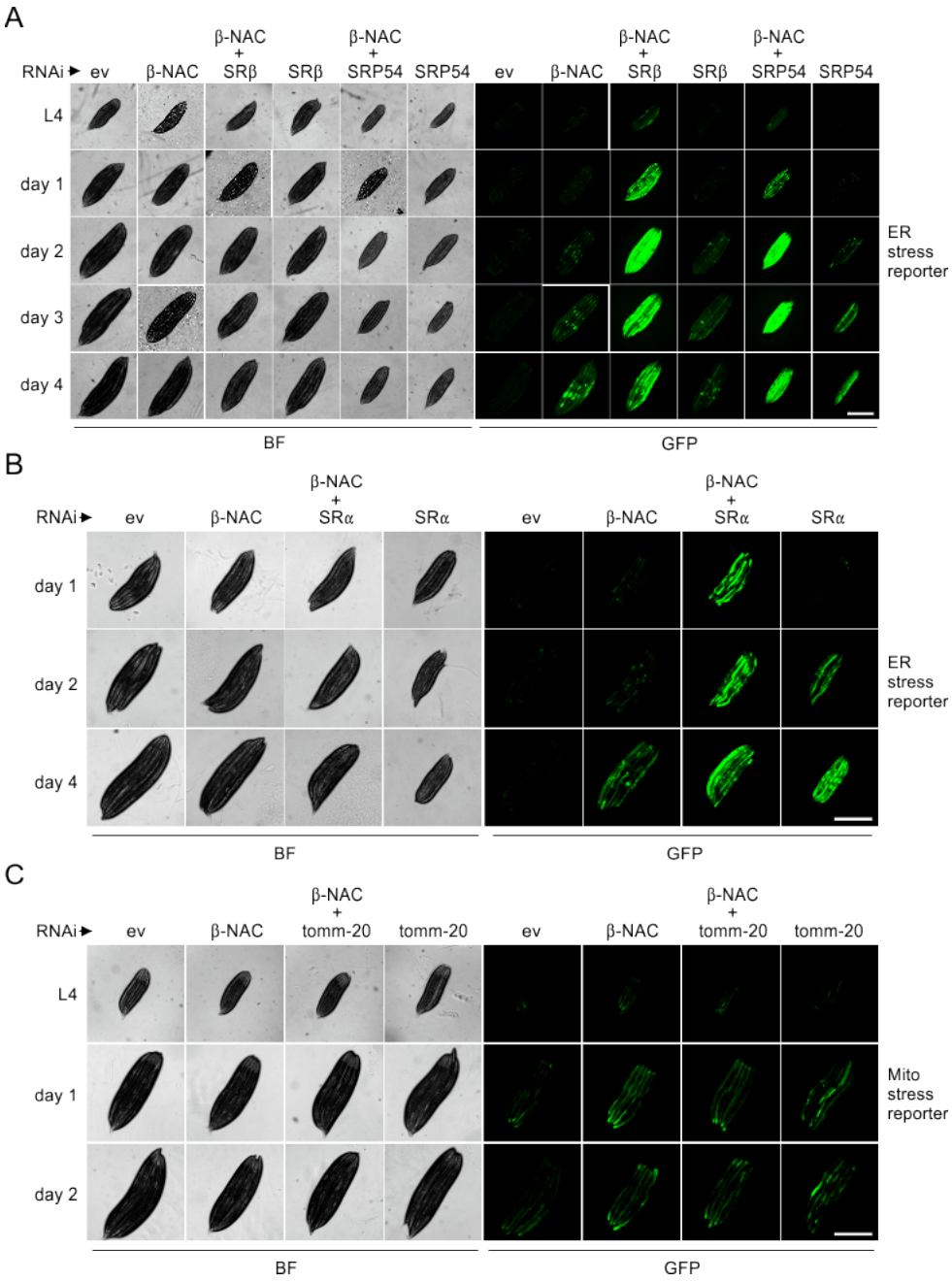

Fig. S2 Impairment of the SRP pathway potentiates the ER stress response in NAC depleted animals.

(**A**) *hsp-4p::GFP* ER stress reporter worms were grown on empty vector control (ev) or indicated RNAi and GFP fluorescence was assessed from the last larval stage (L4) to day 4 of adulthood. (**B**) *hsp-4p::GFP* ER stress reporter worms were grown on empty vector control (ev), β-NAC, β-NAC + SRα, or SRα RNAi and GFP fluorescence was assessed from day 1 to day 4 of adulthood. (**C**) *hsp-6p::GFP* mitochondrial stress reporter worms were grown on empty vector control (ev) or indicated RNAi and GFP fluorescence was assessed from the last larval stage (L4) to day 2 of adulthood. BF = Bright-field. Scale bar = 0.5 mm.

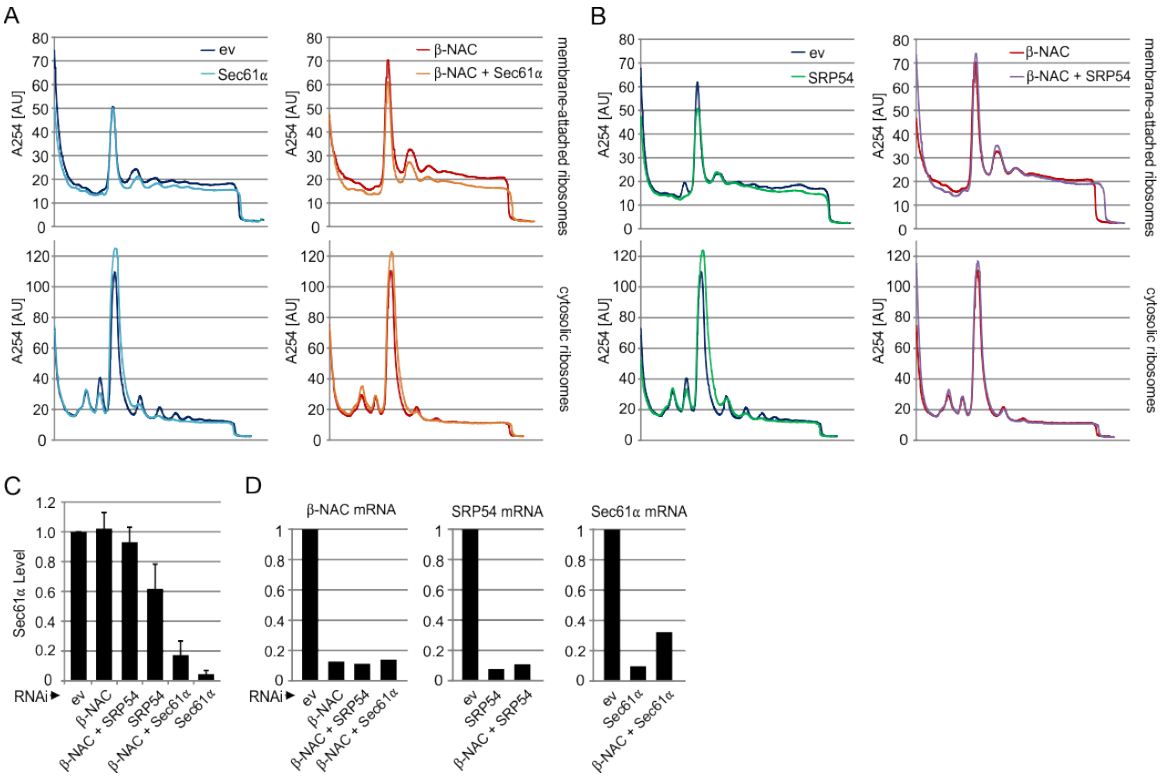

Fig. S3 NAC depletion leads to increased, SRP-independent binding of ribosomes to ER translocons

(**A**) N2 worms were grown on empty vector control (ev, dark blue), Sec61α RNAi (light blue), β-NAC RNAi (red) or β-NAC + Sec61α RNAi (orange). On day 3 of adulthood polysome profiles of membrane-attached (upper panels) and cytosolic (lower panels) ribosomes were assessed. (**B**) N2 worms were grown on empty vector control (ev, dark blue), SRP54 RNAi (green), β-NAC RNAi (red) or β-NAC + SRP54 RNAi (violet). On day 3 of adulthood polysome profiles of membrane-attached (upper panels) and cytosolic (lower panels) ribosomes were assessed. (**C**) Quantification of Sec61α levels assessed by immunoblotting shown as in Figure 2C. Data are represented as mean ± SD. (**D**) Knockdown efficiencies of RNAi experiment shown in Figure 2C measured by means of quantitative RT-PCR.

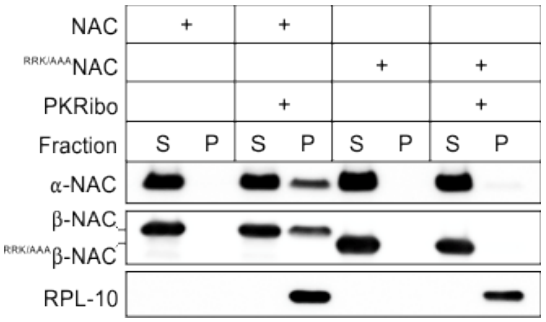

Fig. S4 Ribosome sedimentation assay testing the binding of WT-NAC and $^{RRK/AAA}$-NAC to ribosomes

Puromycin and high salt-stripped ribosomes (PKRibo, 0.5 μM) were incubated with WT-NAC or mutant $^{RRK/AAA}$NAC (8 μM), in which the evolutionary conserved RRK motif in β-NAC, that is critical for ribosome binding (*34*), was mutated to AAA. Ribosomes were pelleted through a sucrose cushion by ultracentrifugation and bound and unbound NAC was assessed in the pellet (P) and supernatant (S), respectively, by immunoblot analysis. Note that $^{RRK/AAA}$β-NAC migrates faster than WT-β-NAC in SDS-PAGE due to charge variation.

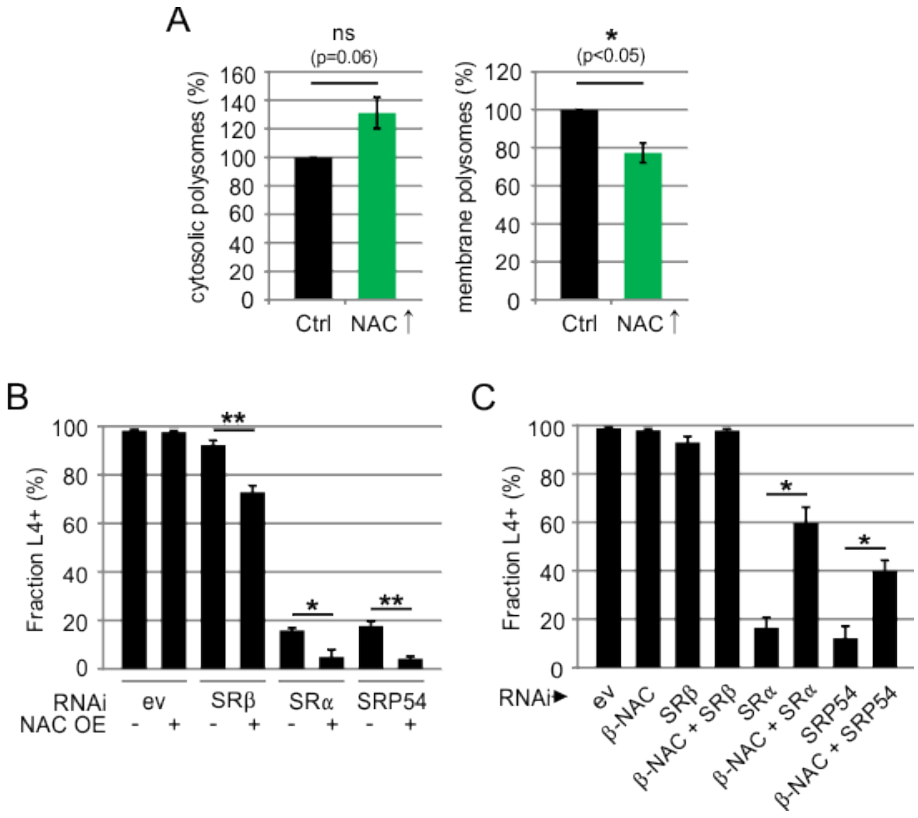

Fig. S5 NAC overexpression interferes with SRP-dependent targeting

(**A**) Polysome quantifications of cytosolic and membrane ribosome profiles of control (Ctrl) and NAC-overexpressing worms (NAC↑) shown as in Fig. 3A, B. Polysomal peaks were quantified using Image J. Data are represented as mean ± SD. A Student's t test was used to assess significance: *p < 0.05; n = 3. ns = not significant. (**B**) Control (-) and NAC overexpressing L1 larvae (+) were grown on empty vector control (ev) or indicated RNAi. After 4 days, the fraction of adult animals (L4+) was assessed. Data are represented as mean ± SD. A Student's t test was used to assess significance: *p < 0.05, **p < 0.01. OE = overexpression. (**H**) N2 worms (L1 larvae) were grown on empty vector control (ev) or indicated RNAi. After 4 days, the fraction of adult animals (L4+) was assessed. Data are represented as mean ± SD. A Student's t test was used to assess significance: *p < 0.05.

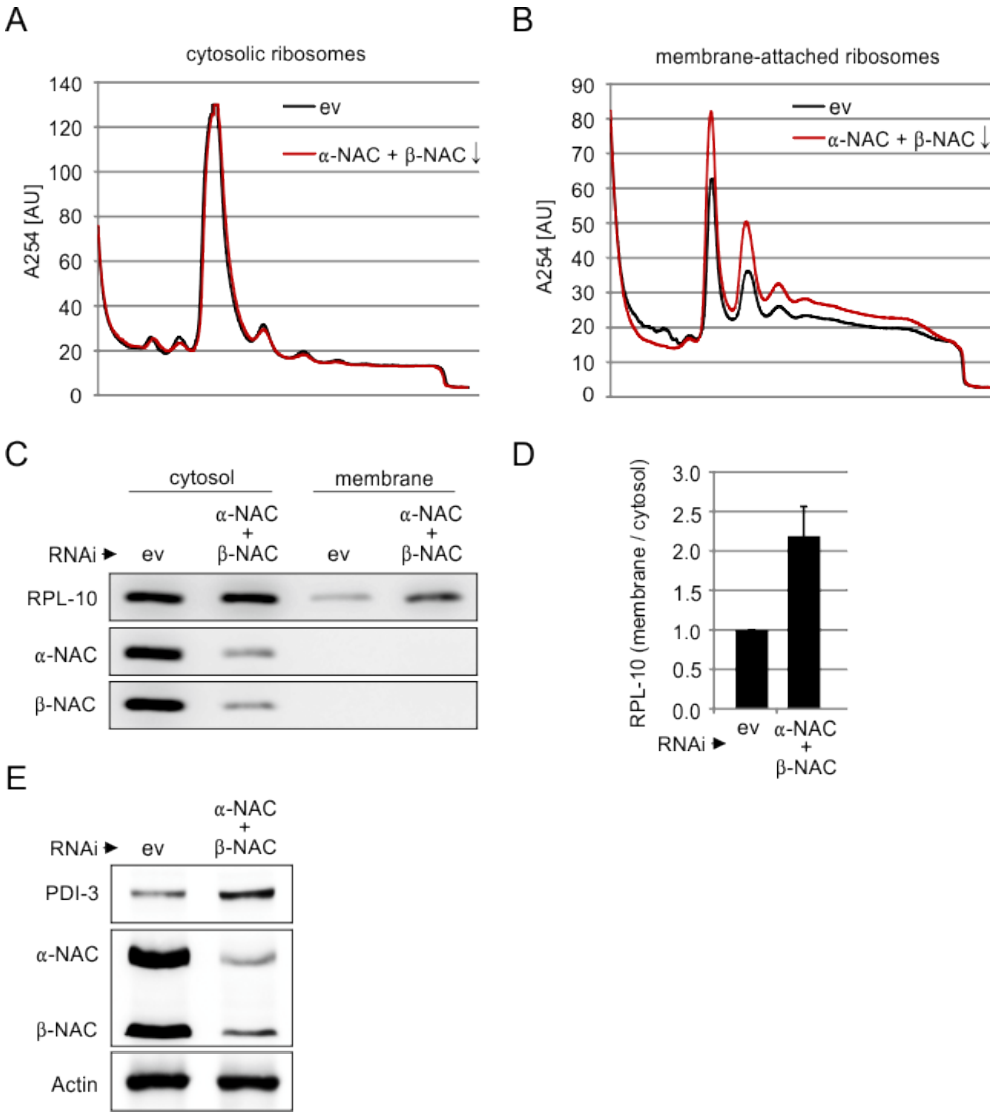

Fig. S6 NAC RNAi phenotype in temperature-sensitive sterile mutants

(A) Temperature sensitive sterile mutants (SS104) were grown at the nonpermissive temperature on empty vector control (ev, black) or α-NAC + β-NAC RNAi (red). On day 3 of adulthood polysome profiles of cytosolic ribosomes were assessed. (**B**) Polysome profile of membrane-attached ribosomes from animals as in (A). (**C**) Ribosomal fractions of sedimentation analyses shown in (A) and (B) were collected and subjected to immunoblot analysis of indicated proteins. (**D**) Diagram shows the membrane-to-cytosol ratio of ribosomes by means of RPL-10 levels in the cytosolic and membrane fractions shown as in (C). Ratio of empty vector control (ev) worms was set to one. Data are represented as mean ± SD. (**E**) Total extracts of animals as in (A) were prepared and indicated proteins were analyzed by immunoblotting. Actin served as loading control.

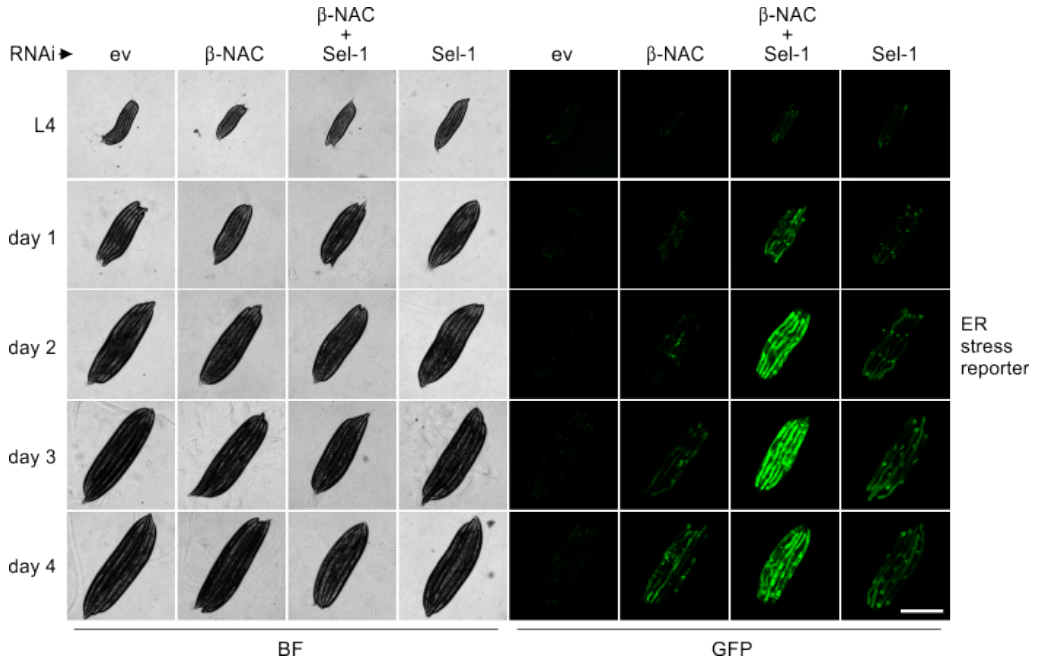

Fig. S7 Impairment of the ERAD pathway increases the ER stress response in NAC depleted animals

hsp-4p::GFP ER stress reporter worms were grown on empty vector control (ev) or indicated RNAi and GFP fluorescence was assessed from the last larval stage (L4) to day 4 adulthood. BF = Bright-field. Scale bar = 0.5 mm.

References and Notes

1. M. Halic, T. Becker, M. R. Pool, C. M. Spahn, R. A. Grassucci, J. Frank, R. Beckmann, Structure of the signal recognition particle interacting with the elongation-arrested ribosome. *Nature* **427**, 808–814 (2004). Medline doi:10.1038/nature02342

2. M. Halic, M. Gartmann, O. Schlenker, T. Mielke, M. R. Pool, I. Sinning, R. Beckmann, Signal recognition particle receptor exposes the ribosomal translocon binding site. *Science* **312**, 745–747 (2006). Medline doi:10.1126/science.1124864

3. Y. Nyathi, B. M. Wilkinson, M. R. Pool, Co-translational targeting and translocation of proteins to the endoplasmic reticulum. *Biochim. Biophys. Acta* **1833**, 2392–2402 (2013). Medline doi:10.1016/j.bbamcr.2013.02.021

4. T. A. Rapoport, Protein translocation across the eukaryotic endoplasmic reticulum and bacterial plasma membranes. *Nature* **450**, 663–669 (2007). Medline doi:10.1038/nature06384

5. T. Schwartz, G. Blobel, Structural basis for the function of the beta subunit of the eukaryotic signal recognition particle receptor. *Cell* **112**, 793–803 (2003). Medline doi:10.1016/S0092-8674(03)00161-2

6. P. Walter, I. Ibrahimi, G. Blobel, Translocation of proteins across the endoplasmic reticulum. I. Signal recognition protein (SRP) binds to in-vitro-assembled polysomes synthesizing secretory protein. *J. Cell Biol.* **91**, 545–550 (1981). Medline doi:10.1083/jcb.91.2.545

7. B. Wiedmann, H. Sakai, T. A. Davis, M. Wiedmann, A protein complex required for signal-sequence-specific sorting and translocation. *Nature* **370**, 434–440 (1994). Medline doi:10.1038/370434a0

8. N. Borgese, W. Mok, G. Kreibich, D. D. Sabatini, Ribosomal-membrane interaction: In vitro binding of ribosomes to microsomal membranes. *J. Mol. Biol.* **88**, 559–580 (1974). Medline doi:10.1016/0022-2836(74)90408-2

9. B. Jungnickel, T. A. Rapoport, A posttargeting signal sequence recognition event in the endoplasmic reticulum membrane. *Cell* **82**, 261–270 (1995). Medline doi:10.1016/0092-8674(95)90313-5

10. K. U. Kalies, D. Görlich, T. A. Rapoport, Binding of ribosomes to the rough endoplasmic reticulum mediated by the Sec61p-complex. *J. Cell Biol.* **126**, 925–934 (1994). Medline doi:10.1083/jcb.126.4.925

11. B. Lauring, H. Sakai, G. Kreibich, M. Wiedmann, Nascent polypeptide-associated complex protein prevents mistargeting of nascent chains to the endoplasmic reticulum. *Proc. Natl. Acad. Sci. U.S.A.* **92**, 5411–5415 (1995). Medline doi:10.1073/pnas.92.12.5411

12. A. Prinz, E. Hartmann, K. U. Kalies, Sec61p is the main ribosome receptor in the endoplasmic reticulum of *Saccharomyces cerevisiae*. *Biol. Chem.* **381**, 1025–1029 (2000). Medline doi:10.1515/BC.2000.126

13. T. A. Bloss, E. S. Witze, J. H. Rothman, Suppression of CED-3-independent apoptosis by mitochondrial betaNAC in *Caenorhabditis elegans*. *Nature* **424**, 1066–1071 (2003). Medline doi:10.1038/nature01920

14. S. L. Rea, D. Wu, J. R. Cypser, J. W. Vaupel, T. E. Johnson, A stress-sensitive reporter predicts longevity in isogenic populations of *Caenorhabditis elegans*. *Nat. Genet.* **37**, 894–898 (2005). Medline doi:10.1038/ng1608

15. Materials and methods are available as supplementary materials on *Science* Online.

16. M. Calfon, H. Zeng, F. Urano, J. H. Till, S. R. Hubbard, H. P. Harding, S. G. Clark, D. Ron, IRE1 couples endoplasmic reticulum load to secretory capacity by processing the XBP-1 mRNA. *Nature* **415**, 92–96 (2002). Medline doi:10.1038/415092a

17. T. Yoneda, C. Benedetti, F. Urano, S. G. Clark, H. P. Harding, D. Ron, Compartment-specific perturbation of protein handling activates genes encoding mitochondrial chaperones. *J. Cell Sci.* **117**, 4055–4066 (2004). Medline doi:10.1242/jcs.01275

18. J. Kirstein-Miles, A. Scior, E. Deuerling, R. I. Morimoto, The nascent polypeptide-associated complex is a key regulator of proteostasis. *EMBO J.* **32**, 1451–1468 (2013). Medline doi:10.1038/emboj.2013.87

19. M. R. Adelman, D. D. Sabatini, G. Blobel, Ribosome-membrane interaction. Nondestructive disassembly of rat liver rough microsomes into ribosomal and membranous components. *J. Cell Biol.* **56**, 206–229 (1973). Medline doi:10.1083/jcb.56.1.206

20. S. S. Vembar, J. L. Brodsky, One step at a time: Endoplasmic reticulum-associated degradation. *Nat. Rev. Mol. Cell Biol.* **9**, 944–957 (2008). Medline doi:10.1038/nrm2546

21. F. Urano, M. Calfon, T. Yoneda, C. Yun, M. Kiraly, S. G. Clark, D. Ron, A survival pathway for *Caenorhabditis elegans* with a blocked unfolded protein response. *J. Cell Biol.* **158**, 639–646 (2002). Medline doi:10.1083/jcb.200203086

22. F. Schwarz, M. Aebi, Mechanisms and principles of *N*-linked protein glycosylation. *Curr. Opin. Struct. Biol.* **21**, 576–582 (2011). Medline doi:10.1016/j.sbi.2011.08.005

23. S. Cabantous, T. C. Terwilliger, G. S. Waldo, Protein tagging and detection with engineered self-assembling fragments of green fluorescent protein. *Nat. Biotechnol.* **23**, 102–107 (2005). Medline doi:10.1038/nbt1044

24. W. Neupert, J. M. Herrmann, Translocation of proteins into mitochondria. *Annu. Rev. Biochem.* **76**, 723–749 (2007). Medline doi:10.1146/annurev.biochem.76.052705.163409

25. O. Yogev, O. Pines, Dual targeting of mitochondrial proteins: Mechanism, regulation and function. *Biochim. Biophys. Acta* **1808**, 1012–1020 (2011). Medline doi:10.1016/j.bbamem.2010.07.004

26. I. Möller, M. Jung, B. Beatrix, R. Levy, G. Kreibich, R. Zimmermann, M. Wiedmann, B. Lauring, A general mechanism for regulation of access to the translocon: Competition for a membrane attachment site on ribosomes. *Proc. Natl. Acad. Sci. U.S.A.* **95**, 13425–13430 (1998). Medline doi:10.1073/pnas.95.23.13425

27. A. Neuhof, M. M. Rolls, B. Jungnickel, K. U. Kalies, T. A. Rapoport, Binding of signal recognition particle gives ribosome/nascent chain complexes a competitive advantage in endoplasmic reticulum membrane interaction. *Mol. Biol. Cell* **9**, 103–115 (1998). Medline doi:10.1091/mbc.9.1.103

28. D. Raden, R. Gilmore, Signal recognition particle-dependent targeting of ribosomes to the rough endoplasmic reticulum in the absence and presence of the nascent polypeptide-associated complex. *Mol. Biol. Cell* **9**, 117–130 (1998). Medline doi:10.1091/mbc.9.1.117

29. M. del Alamo, D. J. Hogan, S. Pechmann, V. Albanese, P. O. Brown, J. Frydman, Defining the specificity of cotranslationally acting chaperones by systematic analysis of mRNAs associated with ribosome-nascent chain complexes. *PLOS Biol.* **9**, e1001100 (2011). Medline doi:10.1371/journal.pbio.1001100

30. B. Reimann, J. Bradsher, J. Franke, E. Hartmann, M. Wiedmann, S. Prehn, B. Wiedmann, Initial characterization of the nascent polypeptide-associated complex in yeast. *Yeast* **15**, 397–407 (1999). Medline doi:10.1002/(SICI)1097-0061(19990330)15:5<397::AID-YEA384>3.0.CO;2-U

31. T. Ast, G. Cohen, M. Schuldiner, A network of cytosolic factors targets SRP-independent proteins to the endoplasmic reticulum. *Cell* **152**, 1134–1145 (2013). Medline doi:10.1016/j.cell.2013.02.003

32. S. C. Mutka, P. Walter, Multifaceted physiological response allows yeast to adapt to the loss of the signal recognition particle-dependent protein-targeting pathway. *Mol. Biol. Cell* **12**, 577–588 (2001). Medline doi:10.1091/mbc.12.3.577

33. R. M. Voorhees, I. S. Fernández, S. H. Scheres, R. S. Hegde, Structure of the mammalian ribosome-Sec61 complex to 3.4 Å resolution. *Cell* **157**, 1632–1643 (2014). Medline doi:10.1016/j.cell.2014.05.024

34. R. D. Wegrzyn, D. Hofmann, F. Merz, R. Nikolay, T. Rauch, C. Graf, E. Deuerling, A conserved motif is prerequisite for the interaction of NAC with ribosomal protein L23 and nascent chains. *J. Biol. Chem.* **281**, 2847–2857 (2006). Medline doi:10.1074/jbc.M511420200

35. M. Pech, T. Spreter, R. Beckmann, B. Beatrix, Dual binding mode of the nascent polypeptide-associated complex reveals a novel universal adapter site on the ribosome. *J. Biol. Chem.* **285**, 19679–19687 (2010). Medline doi:10.1074/jbc.M109.092536

36. Y. Zhang, U. Berndt, H. Gölz, A. Tais, S. Oellerer, T. Wölfle, E. Fitzke, S. Rospert, NAC functions as a modulator of SRP during the early steps of protein targeting to the endoplasmic reticulum. *Mol. Biol. Cell* **23**, 3027–3040 (2012). Medline doi:10.1091/mbc.E12-02-0112

37. U. Raue, S. Oellerer, S. Rospert, Association of protein biogenesis factors at the yeast ribosomal tunnel exit is affected by the translational status and nascent polypeptide sequence. *J. Biol. Chem.* **282**, 7809–7816 (2007). Medline doi:10.1074/jbc.M611436200

38. T. Powers, P. Walter, The nascent polypeptide-associated complex modulates interactions between the signal recognition particle and the ribosome. *Curr. Biol.* **6**, 331–338 (1996). Medline doi:10.1016/S0960-9822(02)00484-0

39. J. M. Deng, R. R. Behringer, An insertional mutation in the BTF3 transcription factor gene leads to an early postimplantation lethality in mice. *Transgenic Res.* **4**, 264–269 (1995). Medline doi:10.1007/BF01969120

40. D. C. Markesich, K. M. Gajewski, M. E. Nazimiec, K. Beckingham, bicaudal encodes the *Drosophila* beta NAC homolog, a component of the ribosomal translational machinery. *Development* **127**, 559–572 (2000). Medline

41. Y. Hotokezaka, K. van Leyen, E. H. Lo, B. Beatrix, I. Katayama, G. Jin, T. Nakamura, alphaNAC depletion as an initiator of ER stress-induced apoptosis in hypoxia. *Cell Death Differ.* **16**, 1505–1514 (2009). Medline doi:10.1038/cdd.2009.90

42. H. Olzscha, S. M. Schermann, A. C. Woerner, S. Pinkert, M. H. Hecht, G. G. Tartaglia, M. Vendruscolo, M. Hayer-Hartl, F. U. Hartl, R. M. Vabulas, Amyloid-like aggregates sequester numerous metastable proteins with essential cellular functions. *Cell* **144**, 67–78 (2011). Medline doi:10.1016/j.cell.2010.11.050

43. R. V. Rao, D. E. Bredesen, Misfolded proteins, endoplasmic reticulum stress and neurodegeneration. *Curr. Opin. Cell Biol.* **16**, 653–662 (2004). Medline doi:10.1016/j.ceb.2004.09.012

44. S. Brenner, The genetics of *Caenorhabditis elegans*. *Genetics* **77**, 71–94 (1974). Medline

45. E. H. Feinberg, M. K. Vanhoven, A. Bendesky, G. Wang, R. D. Fetter, K. Shen, C. I. Bargmann, GFP Reconstitution Across Synaptic Partners (GRASP) defines cell contacts and synapses in living nervous systems. *Neuron* **57**, 353–363 (2008). Medline doi:10.1016/j.neuron.2007.11.030

46. C. C. Mello, J. M. Kramer, D. Stinchcomb, V. Ambros, Efficient gene transfer in *C.elegans*: Extrachromosomal maintenance and integration of transforming sequences. *EMBO J.* **10**, 3959–3970 (1991). Medline

47. A. Krogh, B. Larsson, G. von Heijne, E. L. Sonnhammer, Predicting transmembrane protein topology with a hidden Markov model: Application to complete genomes. *J. Mol. Biol.* **305**, 567–580 (2001). Medline doi:10.1006/jmbi.2000.4315

48. K. Min, J. Kang, J. Lee, A modified feeding RNAi method for simultaneous knock-down of more than one gene in *Caenorhabditis elegans*. *Biotechniques* **48**, 229–232 (2010). Medline doi:10.2144/000113365